INSTITUTE OF PLASMA PHYSICS

NAGOYA UNIVERSITY

RESEARCH REPORT

NAGOYA, JAPAN

Concept for a Double Cusp Fusion Reactor with the Adiabatic RF Plugging

Tadatsugu Hatori

IPPJ-192 June 1974

Further communication about this report is to be sent to the Research Information Center, Institute of Plasma Physics, Nagoya University, Nagoya, Japan.

Synopsis

The adiabatic rf plugging scheme is proved to be efficient enough when it is applied to a cusp system, and a possible prototype of a fusion reactor is sketched. The proposed system is composed of two cylindrically symmetric cusp geometries and a long central section, of about 100 m, connecting them. In the line and the point cusp regions an rf field with the frequency of the order of the ion cyclotron frequency is applied to suppress the end loss. In contrast with the conventional mirrors, the confinement mechanism is independent of ion collisions, so that a moderate plasma temperature, for instance 20 KeV, is allowed, and also the confinement time is proportional to the system length. This scheme has a high purity advantage over the toroidal systems. The frequency of the rf field is properly set so that the rf barrier reflects only deuterons and tritons and is insensitive to heavy impurity ions in the low ionization stage.

§1. Introduction

In this article, the adiabatic rf plugging scheme proposed by Watson[1] is proved to be efficient when it is applied to a cusp system, and a possible prototype of a fusion reactor is given.[2] The present scheme is, as shown in §2, composed of two cylindrically symmetric cusp geometries and a long central section connecting them. Although it is an open-ended system, it does not suffer from the end loss for at least 1 sec and from the micro instabilities. In contrast with conventional mirrors, the confinement mechanism of adiabatic rf plugging is independent of ion collisions, so that a moderate plasma temperature, for instance 20 keV, is allowed, and also the confinement time is proportional to the system length.

One of the purposes of this paper is to give the required strength of the rf field for the confinement of a thermonuclear plasma. The required strength for the rf field is not only determined by the plasma pressure, but also depends on the system length. Larger dimensions require weaker rf fields. If the system length is assumed to be about one hundred meters, it is guaranteed that the strength of rf field is well within the reach of present technology, and satisfies the power balance limitation.

One of the advantages of cusp configuration is that in the line (point) cusp region the width (radius) of the plasma can be reduced down to the order of the ion Larmor radius,[3] which is thin (slender) enough for an eigen mode[4),5] to

exist near the ion cyclotron frequency, so that an external field can penetrate well inside the plasma. To realize this slender plasma in the point cusp region, it is necessary to prevent electrons from streaming back through the line cusp region. As a result of this operation, there occurs a sheath in the outer region of the cusp configuration; the good curvature of the field lines is strengthened in this region so as to suppress an instability originating from the direct radial electric field in the sheath.

It should be noted that impurity ions, α-particles and electrons easily go over the rf barrier. The cyclotron frequencies of impurity ions in the low ionization stage and of electrons are so different from the applied frequency ω which is on order of the deuterium or the tritium cyclotron frequency, that effective potentials for impurity ions and electrons are negligibly small. Loss of α-particles is due to its much higher energy relative to the height of the rf barrier. This scheme therefore retains the high purity advantage of conventional mirror over toroidal system, and a steady operation is possible. The effective potential ψ for ions is reduced to $\frac{T_i}{T_i + T_e}\psi$ by the ambipolar field between electrons and ions of temperatures T_e and T_i, respectively. In this sense T_e is desired to be less than T_i.

The plasma length and density required by this scheme is much less than the corresponding values found for the multiple-mirror.[6] The rf plugging method, where the effective potential is only insensitive to electrons, compares also advantageously with direct potential plugging,[7] which has a negative effect to electrons.

§2. Outline of The Present Scheme

The reactor configuration which is considered here is shown in Fig.1. On both ends of the long straight section there are two cusp configurations. In the line and point cusp field adiabatic rf plugging is applied to suppress the end loss. The plug in the point cusp is not indispensable, if an effecient method is found to prevent electrons from flowing back through the line cusp to the point cusp.[3)]

Concerning the configuration of the magnetic field in the central section, further study is required. The simplest configuraiton would be a straight section. Ideally it could also consist of a multiple mirror (see §6), since a longer life time is expected because of the possibility of trapping particles in a mirror cell. However, the use of shear might be necessary in order to suppress flute and drift instabilities.

Examples of parameters of this reactor system is summarized in Table 1.

§3. Characteristics of The Cusp Field

This section develops a simple theory for the self consistent field in the plasma which clarifies the reason why the width (radius) of the plasma must be of the order of the ion Larmor radius.

We first limit ourselves to the "sheet plasma" in the line cusp. The perpendicular direction to the sheet is the z-axis and the direction of the magnetic field is parallel

to the sheet plane. We consider an idealized situation where the magnetic field is uniform and the system is homogeneous in the perpendicular directions to the z-axis. We consider only the z component of the rf field which is assumed to depend only on z. The excited standing wave by the external field, $E_z = E_{ex} \sin \omega t$, is assumed to be electrostatic.

The most important mode among others for the adiabatic rf plugging is the fundamental mode which has a profile E(z) of standing wave amplitude nearly proportional to the shape of the unperturbed density, $n_0(z)$. For this fundamental mode, the cold treatment for ions is a good approximation.[4] Then we have

$$\frac{\partial}{\partial z} E(z) = 4\pi e \left\{ \frac{\partial}{\partial z} n_{0D}(z) \frac{1}{\omega^2 - \omega_{cD}^2} \frac{e}{M_D} E(z) + \frac{\partial}{\partial z} n_{0T}(z) \frac{1}{\omega^2 - \omega_{cT}^2} \frac{e}{M_T} E(z) - n_e(z) \right\}, \quad (3\text{-}1)$$

where ω_c is the cyclotron frequency, and suffixes D, T, and e indicate the deuteron, the triton and the electron, respectively. And n_e is the perturbed density of electrons.

Integrating the eq.(3-1) with respect of z, and putting $E(z=0) \equiv E_0$, $E(z=\pm 0) = E_{ex}$, we have

$$E_0 - E_{ex} = \left\{ \frac{\omega_{pD}^2(0)}{\omega^2 - \omega_{cD}^2} + \frac{\omega_{pT}^2(0)}{\omega^2 - \omega_{cT}^2} \right\} E_0 - 4\pi e \int_{-\infty}^{0} n_e(z)\, dz . \quad (3\text{-}2)$$

The density $n_e(z)$ is assumed to be the Boltzman distribution,

$$n_e(z) = n_{0e}(z) \frac{e\phi(z)}{T} , \quad (3\text{-}3)$$

where $\phi = \int^{z} E(z')dz'$ is the electrostatic potential. The scale length of the magnetic field is in general much larger than the electron transit length v_{Te}/ω along the lines of force in a period of rf oscillation. The last term on the right hand side of eq.(3-2) is estimated as

$$4\pi e\int_{-\infty}^{0} n_e(z)dz \sim \frac{4\pi(n_{0D}(0)+n_{0T}(0))e^2}{T}\left(\frac{\lambda}{2}\right)^2 E_0, \qquad (3\text{-}4)$$

where λ is the width of the distribution of electrons, in general different from that of sheet plasma.

We have a linear relation

$$E_0 / E_{ex} = \frac{1}{\epsilon}, \qquad (3\text{-}5)$$

where

$$\epsilon = 1 - \left\{ \frac{\omega_{pD}^2(0)}{\omega^2-\omega_{cD}^2} + \frac{\omega_{pT}^2(0)}{\omega^2-\omega_{cT}^2} - \frac{4\pi(n_{0D}(0)+n_{0T}(0))e^2}{T}\left(\frac{\lambda}{2}\right)^2 \right\}. \qquad (3\text{-}6)$$

Equating ε to zero gives an eigen frequency of the sheet plasma in the fundamental mode which is in fairly good agreement with the result based upon the Vlasov equation.[4)]

The results obtained are applied to the real line cusp plasma, then the quantities E_0, $n_{0D}(0)$, $n_{0T}(0)$, ω_{cD}, ω_{cT} and so on become functions of the radial coordinate r, along the magnetic field. The unperturbed density of ions are assumed to be the Boltzmann distribution under the quasipotential, $\psi(r) = \frac{M}{4}\left(\frac{e\,E_0(r)}{M}\right)^2 \frac{1}{\omega^2-\omega_c^2(r)}$;

$$n_{0D}(r) = \bar{n}_D(r)\ \exp\left\{-\frac{M_D}{8T}\left(\frac{eE_0(r)}{M_D}\right)^2 \frac{1}{\omega^2-\omega_{cD}^2(r)}\right\}, \qquad (3\text{-}7)$$

$$n_{0T}(r) = \bar{n}_T(r)\ \exp\left\{-\frac{M_T}{8T}\left(\frac{eE_0(r)}{M_T}\right)^2 \frac{1}{\omega^2-\omega_{cT}^2(r)}\right\}, \qquad (3\text{-}8)$$

For deuteron we assume

$$n_{0D}(r) = 0 \quad \text{for} \quad \omega_{cD}(r) > \omega \ .$$

In the eqs.(3-7,8), $\bar{n}_D$ or $\bar{n}_T$ indicates the density in the absence of rf field. In this section we use a simplified expression (See Appendix)

$$\bar{n}_D(r) = \bar{n}_T(r) = 0.15 \quad n(r=0) \ .$$

Now the system (3-5) through (3-8) can determine the field strength $E_0(r)$ selfconsistently. In Fig.2 the results of computation are shown for parameters given there. The Fig.2 shows such a critical position r_s, the boundaries between the penetrating region, $\varepsilon < 1$, and the screened region, $\varepsilon > 1$.

The equation determining r_s for the case $(\lambda/2\rho_0)^2 < 6/5$ is written as, setting $\varepsilon = 1$,

$$0.15\ \exp\left(-\frac{1}{8}\tilde{E}_{ex}^2 \frac{1}{1-r_s^2}\right)\left\{\frac{1}{1-r_s^2} - \left(\frac{\lambda}{2\rho_0}\right)^2\right\}$$
$$+0.10\ \exp\left(-\frac{1}{12}\tilde{E}_{ex}^2 \frac{1}{1-\frac{4}{9}r_s^2}\right)\left\{\frac{1}{1-\frac{4}{9}r_s^2} - \frac{3}{2}\left(\frac{\lambda}{2\rho_0}\right)^2\right\} = 0, \qquad (3\text{-}9)$$

where $\tilde{E}_{ex} \equiv e E_{ex} / (M_D \omega \sqrt{T/M_D})$, $\rho_0 \equiv \sqrt{T/M_D}/\omega$,
and for $(\lambda/2\rho_0)^2 > 6/5$,

$$\gamma_s = \frac{3}{2}\sqrt{1 - \frac{2}{3}\left(\frac{2\rho_0}{\lambda}\right)^2}. \qquad (3\text{-}10)$$

It is remarkable that this critical value is determined independently of the plasma density. Numerical value is shown in Fig.3 with the parameter $\tilde{E}_{ex}$. Fig.3 shows an important feature that as $\lambda/2\rho_0$ increases r_s does also. For the adiabatic reflection of a deuteron the ratio $(\omega-\omega_{cD})/\omega$ must not be small so that no resonance may take place. In the sense that r_s should be well below unity, such a large $\lambda/2\rho_0$ is prohibited that breaks the requirement.

The limitation of the width λ necessarily imposes an upper bound to the plasma radius, a, in the straight section (see Fig.1). If we assume $\lambda/2\rho_0 \leq 1$, the radius is limited to be[3)]

$$a \leq 2\sqrt{\rho R_0} = 1.6\sqrt{\rho R_L}, \qquad (3\text{-}11)$$

where R_0 is the radius of the deuteron resonance point, $\omega=\omega_{cD}$, and R_L is the triton resonance point, which is chosen to be identical with the point of the maximum magnetic field.

A similar argument is also true for the plasma in the point cusp. It is confirmed that there exists a convenient

eigen mode[5] for the adiabatic rf plugging in a slender plasma provided the radius is of the order of the ion Larmor radius.

§4. Computation of Confinement Time

§4-1. Loss Mechanism

We assume that the particle loss and the energy loss across the line of force can be negligible. The energy space ($K_{\parallel}$, $K_{\perp}$), the parallel and perpendicular components, of a particle is divided into five regions in Fig.4 according to the different processes of end loss. The dotted line indicates the loss cone in the absence of rf field. In the presence of rf field the region (1) is the modified loss cone, which should be called the "loss hyperboloid".[8)9)] The region (2) is the nonadiabatic reflection region, where the energy of a particle increases after a reflection due to the rf resonance effect. After the reflection by the rf barrier, the particle goes through the cusp center or flies through the long central section (see Fig.1), and suffers deflections due to the magnetical nonadiabaticity or collisions. Hence the particle will jump to another point on the line, $K_{\parallel}+K_{\perp}$ =const., in ($K_{\parallel}$, $K_{\perp}$) space. The loss process of particles in the region (2) is relatively fast due to the rf resonance heating and deflections. The line, a), drawn between the regions (2) and (3) or (4) distinguishes roughly between the adiabatic and the nonadiabatic reflections. The line a) is given by

$$K_{\parallel} = W_c + \left(\frac{B_0}{B} - 1\right) K_{\perp} , \qquad \text{a)}$$

where B_0 and B are the strength of the magnetic field at a

point of resonance, $\omega=\omega_c$, and the starting point of a particle, respectively. The critical energy,[9] W_c, has an important meaning, the height of the rf barrier, and is given by

$$W_c = \frac{5}{2^{21/5}} M\omega^2 R_0^2 \left(\frac{eE_0}{M\omega^2 R_0}\right)^{8/5}, \qquad (4\text{-}1)$$

R_0 being already defined and having a meaning of the scale length of the curvature of the magnetic field. Particles in the region (3) drop easily into the loss hyperboloid either directly or through the region (2) owing to the deflections. Particles in the region (4) are first deflected into the region (2), then they are heated and finally deflected into the loss hyperboloid. The region (5) is different from the others in the sense that the life time of a particle in this region is much larger than in the others. Particles of energy below W_c remain always below the line a), even after many deflections. The main mechanism of particle loss from the region (5) is the infinitesimal increase of the particle energy due to the small imperfection in the reversibility of the rf barrier.

We divide the loss mechanisms into two categories. I) the fast process which concerns the particle with energy W higher than W_c, $W > W_c$, the regions (1) through (4), and II) the slow process which concerns the particles with $W < W_c$, the region (5). Now the confinement time of the plasma, τ, is composed of two contributions, the fast process confinement time, τ_F, and the slow process one, τ_s, in such a way that

$$\frac{1}{\tau} = \frac{1}{\tau_F} + \frac{1}{\tau_s} . \qquad (4\text{-}2)$$

The value of τ_F can be estimated as

$$\tau_F \sim \frac{\bar{n} V}{n_L v_T S_L} , \qquad (4\text{-}3)$$

where $\bar{n}$ and n_L mean the overall averaged density and the density at the line cusp, V the plasma total volume, v_T thermal velocity of ion, and S_L the total area of the exit of the plasma in the line cusp. The end loss through the point cusp has been assumed to be negligible, because the area of the plasma in the point cusp is generally much smaller than S_L. We assume the ratio $n_L/\bar{n}$ to be maintained as

$$\frac{n_L}{\bar{n}} = 0.3 \exp\left(-W_c/2T\right) . \qquad (4\text{-}4)$$

It may be an over estimate since the number of particles near the energy W_c decreases gradually in the process of confinement relative to the initial Maxwellian value. As $V \sim \pi a^2 L$, where $a \sim 2\sqrt{\rho R_0}$ given by (3-11), and $S_L \sim 4\pi R_0 \Delta\ell$, where $\Delta\ell$ is the width of the sheet plasma given by $4\rho_0$ corresponding to, a, given above, then, using (4-4)

$$\tau_F \sim \frac{L}{v_T} I_F \qquad (4\text{-}5)$$

where

$$I_F \sim \frac{3}{4} \frac{B_0}{B} \exp\left(\frac{W_c}{2T}\right) , \qquad (4\text{-}6)$$

and B_0 and B are the strength of the magnetic field at $r=R_0$ and at the central section, respectively.

In the slow process, the particle end loss is due to the small imperfection in the reversibility of the rf barrier. Let I be the average counts of reflections of a particle before it goes over the rf barrier, then τ_s can be estimated as

$$\tau_s \sim \frac{L}{v_T} I \tag{4-7}$$

or $$\tau_s \sim 10^{-6} L \sqrt{\frac{20}{T}} I ,$$

in the conventional units τ_s(sec), L(m), T(keV). The value, I,will be given in §4-3 by a kind of numerical experiment.

§4-2. Basic Theory of Adiabatic Motion

Before we proceed to compute the value I, we must remember the theory of adiabaticity in the inhomogeneous magnetic field under the rf electric field. The necessary and sufficient conditions[9] for the adiabatic motion are given in the line cusp field,

$$|\dot{\omega}_c(r)| / \omega_c^2(r) \ll 1, \tag{4-8}$$

$$\left| \frac{\dot{r}}{\omega + \omega_c} \frac{1}{E(r)} \frac{d}{dr} E(r) \right| \ll 1, \tag{4-9}$$

$$|\dot{\omega}_c(r)| / (\omega - \omega_c(r))^2 \ll 1, \tag{4-10}$$

$$\bar{\rho} \equiv \rho_0 / R_0 = \sqrt{\frac{T}{M}} \frac{1}{\omega} / R_0 \ll 1, \tag{4-11}$$

$$\bar{E}(r) \equiv eE(r) / M\omega^2 R_0 \ll 1, \tag{4-12}$$

$$R_0 \frac{d}{dr} \bar{E}(r) \ll 1. \tag{4-13}$$

The conditions (4-8) and (4-11) hold also in the absence of rf field. The conditions (4-9) and (4-13) concern with the characteristic length scale for the rf field. Nonresonance condition (4-10) yields the boundary line a) between the adiabatic and nonadiabatic reflection. To get a long confinement time, it is at least necessary that most particles in the Maxwellian distribution have an energy below the critical energy W_c, so that

$$\tilde{T} \equiv \frac{T}{W_c} \ll 1. \tag{4-14}$$

In terms of R_0, E_0, and B_0, suffixes zero referring to the resonance point, $\omega=\omega_c$, we may write the condition (4-11), (4-12) and (4-14) as

$$\bar{\rho} = 2\times 10^{-2}\,(R_0B_0)^{-1}\sqrt{T/20}\,, \tag{4-15}$$

$$\bar{E}_0 = 2.1\,(R_0E_0)(R_0B_0)^{-2}, \tag{4-16}$$

$$\tilde{T} = 4.8\times 10^{-4}\,(R_0B_0)^{6/5}(R_0E_0)^{-8/5}(T/20), \tag{4-17}$$

in the units R_0(m), B_0(10^4G), E_0(MV/cm), T(KeV). In Fig.5 the parameters $\tilde{T}$ and $\bar{E}_0$ are shown in (R_0B_0, R_0E_0) space.

§4-3. Computation of I

The form of the rf field in the plasma is given in §3, but it is too complicated for a numerical computation of I. A simplified but reasonable form is assumed in the following; the electrostatic potential ϕ is assumed to take the form,[9)]

$$\phi(r,z,t) = -E_0 F(r) G_T(r,z) \sin(\omega t+\varphi), \tag{4-18}$$

where

$$F(r) = \begin{cases} 0 & , \ \frac{r}{R_0} < 0.5 , \\ 7.5\left(\frac{r}{R_0}-0.5\right)-250\left(\frac{r}{R_0}-0.6\right)^3-0.25, & 0.5<\frac{r}{R_0}<0.7, \\ 1 & , \ 0.7 < \frac{r}{R_0} , \end{cases} \tag{4-19}$$

and

$$G(r,z) = \epsilon z - \frac{2\rho_0 R_0}{r}(\epsilon-1)\tanh\left(zr/2\rho_0 R_0\right). \tag{4-20}$$

The parameters E_0, ε have the same meaning as in §3, but here the dependence of ε on r is completely neglected.

The process of computing the value of I is a kind of computer simulation. We limit ourselves to the line cusp rf barrier.* In the first place consider a particle at the starting point $r=r_1$, where the rf field vanishes, with the initial conditions, the parallel energy $K_{\parallel}^{(1)}$, the perpendicular energy $K_{\perp}^{(1)}$, the phase of the rf field $\phi^{(1)}$ and the phase of gyration of the particle $\theta^{(1)}$. This particle starts toward the rf barrier and comes back to the initial point with the final energies $K_{\parallel}^{(1)'}$, $K_{\perp}^{(1)'}$. In the second place it starts with the initial conditions, $K_{\parallel}^{(2)}$, $K_{\perp}^{(2)}$, $\phi^{(2)}$, $\theta^{(2)}$, where

---

* The case of the point cusp rf barrier is qualitatively the same except for the value of p_θ, the angular momentum around the symmetry axix, is not conserved but its variance is reversible in the adiabatic reflection case.

the energy conservation, $K_{\parallel}^{(1)'} + K_{\perp}^{(1)'} = K_{\parallel}^{(2)} + K_{\perp}^{(2)}$, is satisfied, and the ratio $K_{\parallel}^{(2)}/K_{\perp}^{(2)}$, $\phi^{(2)}$ and $\theta^{(2)}$ are determined by random numbers. This process of numerical computation of a particle trajectory is continued to the final (I-th) place in which the particle goes out of the rf barrier owing to the increased energy transferred by the rf field.

It is shown in Fig.6 that the total kinetic energy of a test particle fluctuates but the average value increases gradually in the initial and the middle stage, and abruptly in the final stage. In the table 2, various results are summarized.

§5. Power Balance and Scaling

The power plant of this scheme is shown schematically in Fig.7. A different point from the conventional mirror plant is the existence of the rf oscillator. It transfers its energy to the injected plasma with temperature T_0 resulting in the final temperature $\alpha_{RF}\, T_0$, while its energy is dissipated in the rate P_ℓ on the wall of the rf electrodes. It is necessary to limit P_ℓ within a level to be compensated by the fusion power. In Fig.7 the efficiencies of each subsystem η or power P are defined by each suffixes. The heating process of plasma by the fusion product, α-particle, is negligible, since its energy is much higher than the height of rf barrier and its life time is short. It can achieve a positive power balance without the use of direct conversion,

in which case the following treatment holds if we put $\eta_D=\eta_T$.

The net output power P_N of the plant can be written in terms of Q defined by

$$Q \equiv \frac{P_F}{P} = \frac{\text{Fusion power produced in the plasma and blanket}}{\text{Power absorbed by the plasma}}, \quad (5\text{-}1)$$

in the form, $$P_N = \eta_{em}(Q - Q_c)P \quad (5\text{-}2)$$

Here the effective conversion efficiency η_{em} is

$$\eta_{em} = h\eta_T + (1-h)\eta_D \quad (5\text{-}3)$$

and h=0.84 for the D-T reaction and blanket system; we designate Q_c the critical value for Q defined by

$$Q_c \equiv \frac{1-\eta_I\eta_D + \eta_I(\eta_D-\eta_T)r - (1-\eta_I)\eta_T}{\eta_I\eta_{em}}, \quad (5\text{-}4)$$

together with $r \equiv P_R/P$, the portion of the radiation loss.

The condition for positive net output power, $Q > Q_c$, can be rewritten in the form

$$Q = \frac{n\tau}{\alpha_{RF}} 4\times 10^{-14} \frac{\overline{\langle\sigma v\rangle}}{\langle\sigma v\rangle_{20}} \frac{1}{1+\frac{r_0}{\alpha_{RF}}} > Q_c. \quad (5\text{-}5)$$

Here $\langle\sigma v\rangle_{20}$ indicates the average value of σv over the Maxwellian distribution of the injected temperature T_0=20 keV and $\overline{\langle\sigma v\rangle} \equiv \int_{T_0}^{\alpha_{RF}T_0} \langle\sigma v\rangle(T)dT/(\alpha_{RF}-1)T_0$. The factor r_0, the ratio of radiation loss power to the injected power $3nT_0V/\tau$, is given by

$$r_0 \equiv \frac{P_R}{3nT_0V/\tau}$$

$$= 0.24\sqrt{\frac{20}{T(keV)}}\,\frac{n\tau(cm^{-3}sec)}{10^{14}} + 0.13\,\tau(sec)B^2(10kG), \quad (5\text{-}6)$$

due to the bremsstrahlung and synchrotron radiation loss in the single particle theory. In the ordinary situation considered, r_0 is negligibly small. It is noted that the quantity Q_c also depends on n and τ.

The power dissipations in the rf system are due to the losses in the rf oscillator (efficiency η_{os}) and the loading power P_ℓ on the surface of electrodes for plugging. The effective input efficiency of the rf system, η_{RF}, is given by

$$\frac{1}{\eta_{RF}} = \frac{1}{\eta_{os}}\left\{1 + \frac{P_\ell}{(\alpha_{RF}-1)3nT_0V/\tau + P_R}\right\}, \quad (5\text{-}7)$$

V being the plasma total volume. As the loading in the rf electrodes in the line cusp part contributes mainly, we have

$$P_\ell = \frac{1}{2}\frac{E_s^2}{8\pi} S\,\omega\,\delta, \quad (5\text{-}8)$$

where E_s the strength of rf field on the surface of the wall, ω the applied frequency, S the total surface area of the rf electrodes and δ the skin depth. We have considered only the contribution from the line cusp electrodes, since S in the line cusp is much larger than in the point cusp.

It is not difficult to derive the relation among the efficiencies, η_I, η_{RF} and heating efficiency η_H. We have

$$\frac{1}{\eta_I} = \frac{1-r}{\alpha_{RF}} \frac{1}{\eta_H} + \left(1 - \frac{1-r}{\alpha_{RF}}\right) \frac{1}{\eta_{RF}} \quad . \tag{5-9}$$

We finally obtain the upper limit for the loading power P_ℓ owing to (5-4), (5-5), (5-7) and (5-9). In the limit, $r \to 0$ and $\alpha_{RF} \to 1$,

$$\frac{1-\eta_T}{\eta_{os}} P_\ell < \eta_{em} P_F + \left(\eta_D - \frac{1}{\eta_H} - \eta_T\right) 3nT_0 V/\tau \tag{5-10}$$

or

$$\frac{1-\eta_T}{\eta_{os}} \frac{P_\ell}{3nT_0 V/\tau} < \frac{n\tau}{0.25 \times 10^{14}} \eta_{em} + \eta_D - \frac{1}{\eta_H} - \eta_T \, . \tag{5-10}'$$

If one uses superconducting cavities, this condition is easily satisfied. Maintaining a superconducting surface is not impossible because it does not face directly a thermonuclear plasma. It is also possible to satisfy (5-10) for the ordinary cavity, by the sufficient scaling up. The third example in Table 1 is the case.

We briefly discuss the problem of scaling up. Dependence of the confinement time on rf field strength E_{ex}, magnetic field strength in the line cusp B_L and the radius of the ring electrode R_L is only in terms of the arguments $R_L B_L$ and $R_L E_{ex}$. Therefore by increasing the dimensions of the cusp region it is possible to reduce the strength of the magnetic field in the line cusp and the rf electric field. It is

obvious that the confinement time is proportional to the scale length L in the straight region. Increased values of R_L allow larger values of the radius, a, in the central region (see (3-11)), consequently the larger scale of R_L and L has the advantage to allow a larger power output. A larger plasma volume increases fusion power P_F, while the loading P_ℓ is maintained constant if $R_L E_{ex}$ is fixed, so that the condition (5-10) is necessarily satisfied above a critical dimension.

§6. Effect of the Multiple-Mirror

If the multiple-mirror configuration is used for the straight region, the confinement time will be enlarged, since there occurs a possibility of trapping of the particle in the mirror cell. We first introduce the mean free (untrapped by the mirror) path ℓ, mean free time τ_f and mean trapped time τ_t; ℓ is defined by $\ell = v_T \tau_f = v_T \tau_\theta \theta_{\ell c}^2$, $\theta_{\ell c}$ being loss cone angle, and $\tau_\theta = n v_T (2\pi Z^2 Z_0{}^2 e^4 / T^2) \ell n \Lambda$, the Spitzer time for a deflection $\theta^2 = 1$.

We limit ourselves to the case of long mean free path, $L \ll \ell$. A particle flies freely for the time τ_f and is captured in one of the mirror cells for τ_t. Through this unit process, $\frac{\ell}{L}$ times reflections by the rf barrier take place. As the mean reflection counts before loss is denoted by I, $\frac{L}{\ell} I$ repetitions of the process are allowed. Thus a rough estimation of a confinement time τ is

$$\tau \sim (\tau_f + \tau_t) \frac{L}{\ell} I = \frac{\tau_f + \tau_t}{\tau_f} \frac{L}{v_T} I . \qquad (6\text{-}1)$$

The inverse of the improvement factor $(\tau_f + \tau_t)/\tau_f$ is given by

$$\frac{\tau_f}{\tau_f+\tau_t} = \frac{\text{effective loss-cone phase space area}}{\text{total phase space area}} = \frac{1}{\ell_c}\int_0^{\ell_c}\left[1-\sqrt{1-\frac{B(z)}{B_{MAX}}}\right]dz, \quad (6\text{-}2)$$

where ℓ_c is the length of a mirror cell.

Acknowledgements

The author is grateful to Prof. K. Takayama for his suggestion of this problem and continual encouragement, to Prof. T. Sato for his useful comments about the power balance problem, to Dr. J. Jacquinot for his valuable comments about the impurity problem and others and correcting English of the manuscript, and to other theoretical and experimental members of this problem for stimulating discussions.

Appendix Steady Density Distribution in the Line Cusp Region

The distribution function of the plasma in the line cusp region is determined by that of the plasma in the straight section, where the plasma is produced and its distribution function assumes the form

$$f \propto \exp\left(-\frac{M}{2T}v^2\right)\exp\left(-\frac{R^2}{a^2}\right).$$

Here R is the radial coordinate of the gyration center of a particle given by[3)]

$$R^2 = \rho^2 + \frac{2P_\theta}{M\omega_c}, \tag{A1}$$

where ρ and ω_c are the Larmor radius and the cyclotron frequency in the straight section, and P_θ is the angular momentum around the symmetry axis. The quantity, a, is the radius of the plasma given by $a^2 = 4R_0\rho$ due to the inequality (3-11).

The distribution function in the line cusp region in the presence of the rf electric field is given by

$$f \propto \exp\left\{-\frac{M}{2T}(v_r^2+v_z'^2+v_\theta'^2)-\frac{\psi(r)}{2T}\right\}\exp\left(-\frac{2P_\theta}{M\omega_c a^2}\right), \tag{A-2}$$

where the ambipolar effect between ions and electrons is accounted under the condition $T_i=T_e=T$. Modified expressions in the presence of the rf field are given by

$$v_z' = v_z + \frac{\omega}{\omega^2 - \omega_c^2(r)} \frac{eE(r)}{M} \cos(\omega t + \varphi),$$

$$v_\theta' = v_\theta + \frac{\omega_c(r)}{\omega^2 - \omega_c^2(r)} \frac{eE(r)}{M} \sin(\omega t + \varphi),$$

$$P_\theta = Mr\left(v_\theta' - \omega \frac{r}{R_o} \tilde{z}\right),$$

$$\tilde{z} = z + \frac{1}{\omega^2 - \omega_c^2(r)} \frac{eE(r)}{M} \sin(\omega t + \varphi).$$

According to (A1), R^2 must be positive, then the integral region of v'_θ is limited to be

$$v_\theta' \geq \omega \frac{r}{R_o} \tilde{z} - \frac{1}{2} \frac{\omega_c}{r} \rho^2.$$

After integration (A2) over v_r, v'_z and v'_θ, we have finally

$$n(r, \tilde{z}) = \frac{n(r=0)}{\sqrt{\pi}} \exp\left\{\frac{1}{2} \frac{r^2}{R_o^2} \left(\frac{\tilde{z}}{\rho_o} + \frac{1}{4}\right)\right\} \int_{x_o}^{\infty} dx \exp(-x^2),$$

where $x_o = \frac{1}{\sqrt{2}} \left(\frac{\tilde{z}}{\rho_0} + \frac{1}{2}\right) \frac{r}{R_0} - \frac{1}{2\sqrt{2}} \frac{\rho}{r}$. This expression shows $n = 0.3\ n(r=0)$, for $\tilde{z}=0$ and $r=R_o$.

References

1) C.J.H. Watson, Report of the European Controlled Fusion Advisory Group on Open Adiabatic Configuration and RF Plugging, II. C2-a (Dec. 1971).

2) T. Hatori, S. Hiroe, A. Miyahara, T. Sato, K. Takayama, T. Watanabe and T. Watari, Culham Work Shop Report, 1974, Paper No.7, and Proceeding of the First Topical Meeting on the Technology of Controlled Nuclear Fusion, April 16-18, 1974, SanDiego.

3) T. Hatori, Res. Rep. of the Inst. Plasma Phys., Nagoya Univ., Nagoya, Japan, IPPJ-171 (1973).

4) T. Watanabe and T. Hatori, Res. Rep. of the Inst. Plasma Phys., Nagoya Univ., Nagoya, Japan, IPPJ-132 (1972).

5) T. Hatori and T. Watanabe, Res. Rep. of the Inst. Plasma Phys., Nagoya Univ., Nagoya, Japan, IPPJ-133 (1972).

6) R.F. Post, Phys. Rev. Letters 18, 232 (1967)
B. Grant Logan et al., Phys. Rev. Letters 28, 144 (1972),
J.M. Dawson, Meeting of American Physical Society
Nov. 1973, 4A2.

7) P.W. Moir, W.L. Barr and R.F. Post, Phys. of Fluids 14, 2531 (1971).

8) C.J.H. Watson and L.G. Kuo-Petravic, Phys. Rev. Letters, 27, 1231 (1968).

9) T. Hatori and T.Watanabe, Res. Rep. of the Inst. Plasma Phys., Nagoya Univ., Nagoya, Japan, IPPJ-182 (1974).

Figure Caption

Table 1. Various parameters for the fusion reactor.

Table 2. Numerical results for the count of reflections by the rf barrier.

Fig. 1. Double cusp fusion reactor with the adiabatic rf plugging scheme.

Fig. 2. Penetration of the rf field in the line cusp region. The rf field strength in the plasma is obtained as the function of the parallel coordinate r along the magnetic field with the parameter λ, the width of the sheet plasma.

Fig. 3. The relation between the plasma width, λ, and the critical screening point, r_s, above which the external rf field penetrates well and below which it is screened.

Fig. 4. Five regions in $(K_{\parallel}, K_{\perp})$ space. The region (1) is the loss-hyperbloid. The loss process in the regions (2) through (4) is rather fast due to the rf resonance effects or the deflections. Particles in (5) have a long life time.

Fig. 5. Graph of the small parameters $\tilde{T}$ and $\bar{E}_0$. The marked point A corresponds to our design shown in table 1.

Fig. 6. Variation of a particle energy in each reflection by the rf barrier for various cases. Results are summarized in Table 2.

Fig. 7. Power plant of this scheme.

	case 1	Case 2	Case 3
$T_i = T_e$ (keV)	20	20	20
$n(10^{14}cm^{-3})$	1	1	4
τ (sec)	1	1	1
β	0.4	0.4	0.4
E_{ex} (MV/cm)	0.45	0.09	0.09
B (10 kG)	2	2	4
B_L (10 kG)	15	3	3
L (m)	100	100	100
R_L (m)	3	15	15
a (cm)	28	62	44
ρ (cm)	1	1	0.5
P_F (MW)	160	810	6500

Table 1.

I	$\tilde{K} \equiv K/W_c$	$\bar{E}_0 \equiv eE_0/(M\omega^2 R_0)$	$\bar{\rho} \equiv \rho_0/R_0$	ε	R_0E_0 (m MV/cm)	R_0B_0 (m 10kG)
100	10^{-2}	10^{-2}	1.3×10^{-3}	2	1.15	15.5
1500	2×10^{-2}	0.5×10^{-2}	10^{-3}	2	0.9	20
1800	10^{-1}	10^{-2}	4×10^{-3}	1	0.12	5
6000	10^{-2}	10^{-2}	1.3×10^{-3}	1	1.15	15.5
> 5000	10^{-2}	10^{-2}	1.3×10^{-3}	0.5	1.15	15.5
> 10000	2×10^{-2}	0.5×10^{-2}	10^{-3}	1	0.9	20

Table 2.

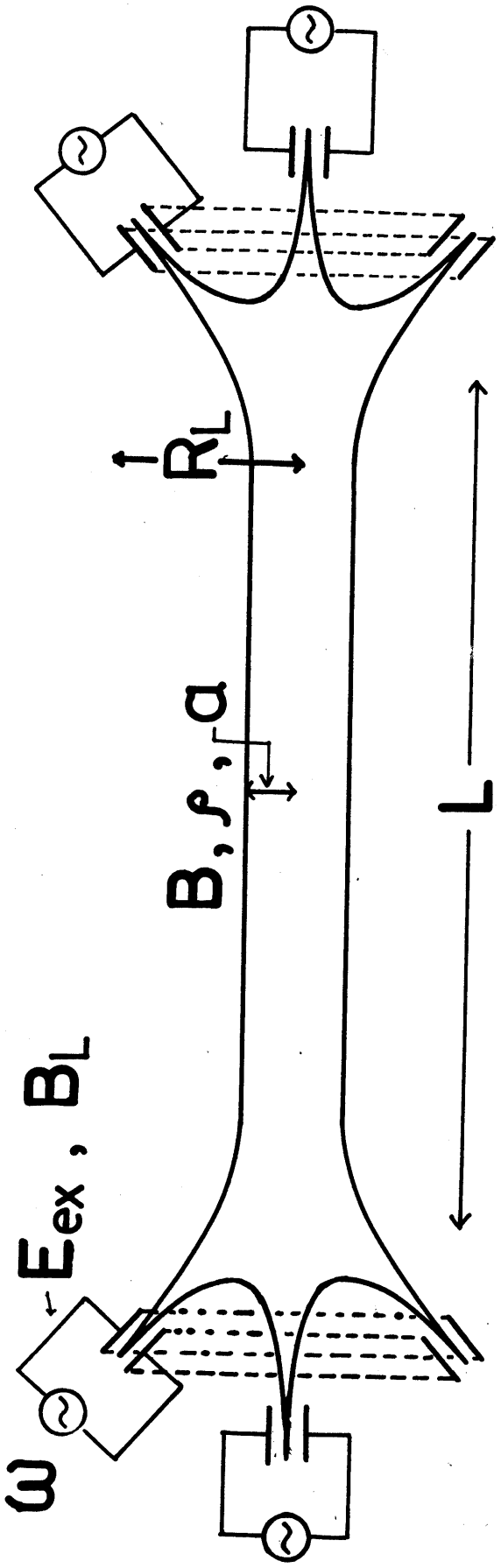

FIG. 1

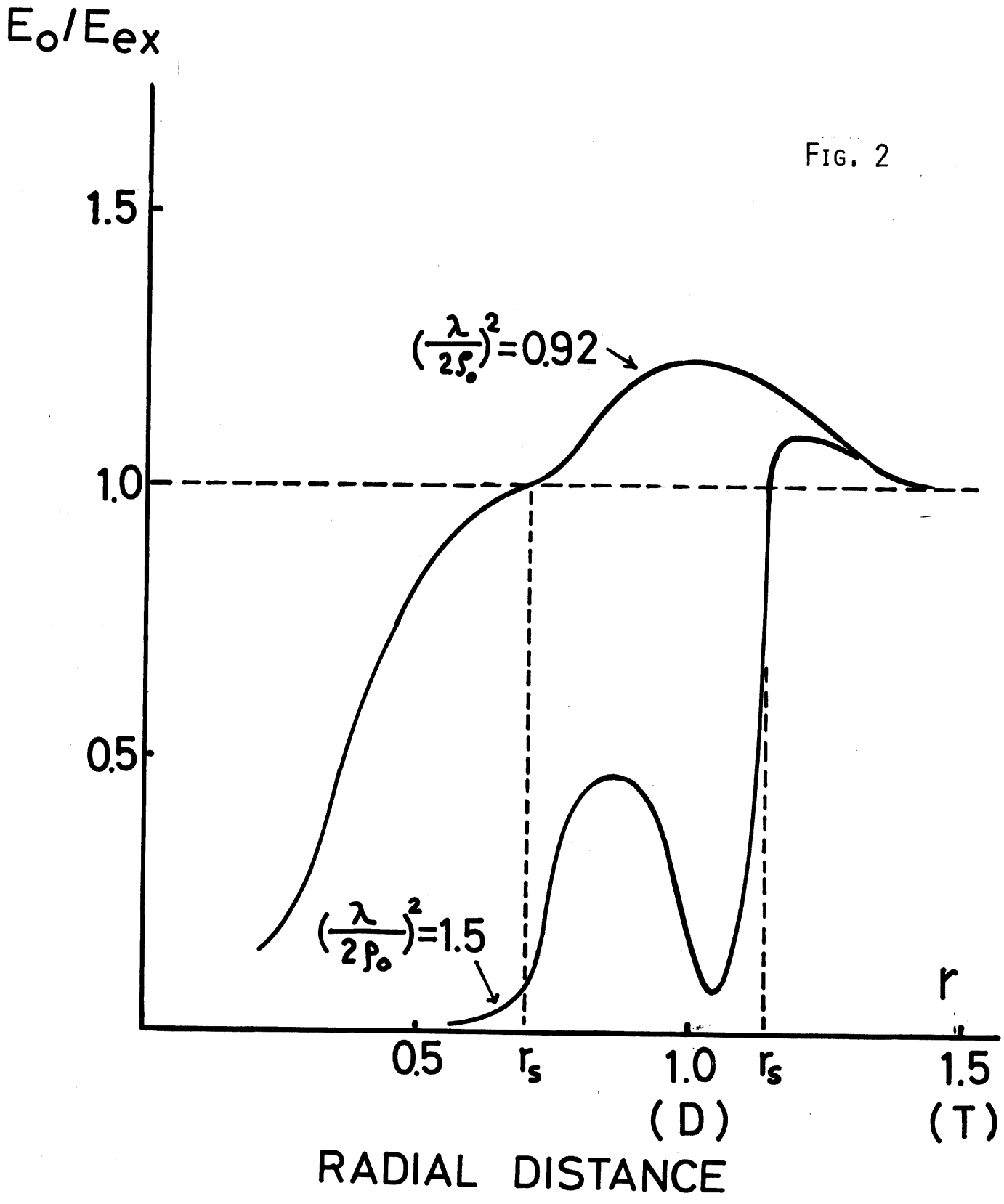
E_o/E_{ex}
1.5
1.0
0.5
$(\frac{\lambda}{2\rho_o})^2=0.92$
$(\frac{\lambda}{2\rho_o})^2=1.5$
r
0.5
r_s
1.0
(D)
r_s
1.5
(T)
RADIAL DISTANCE

FIG. 2

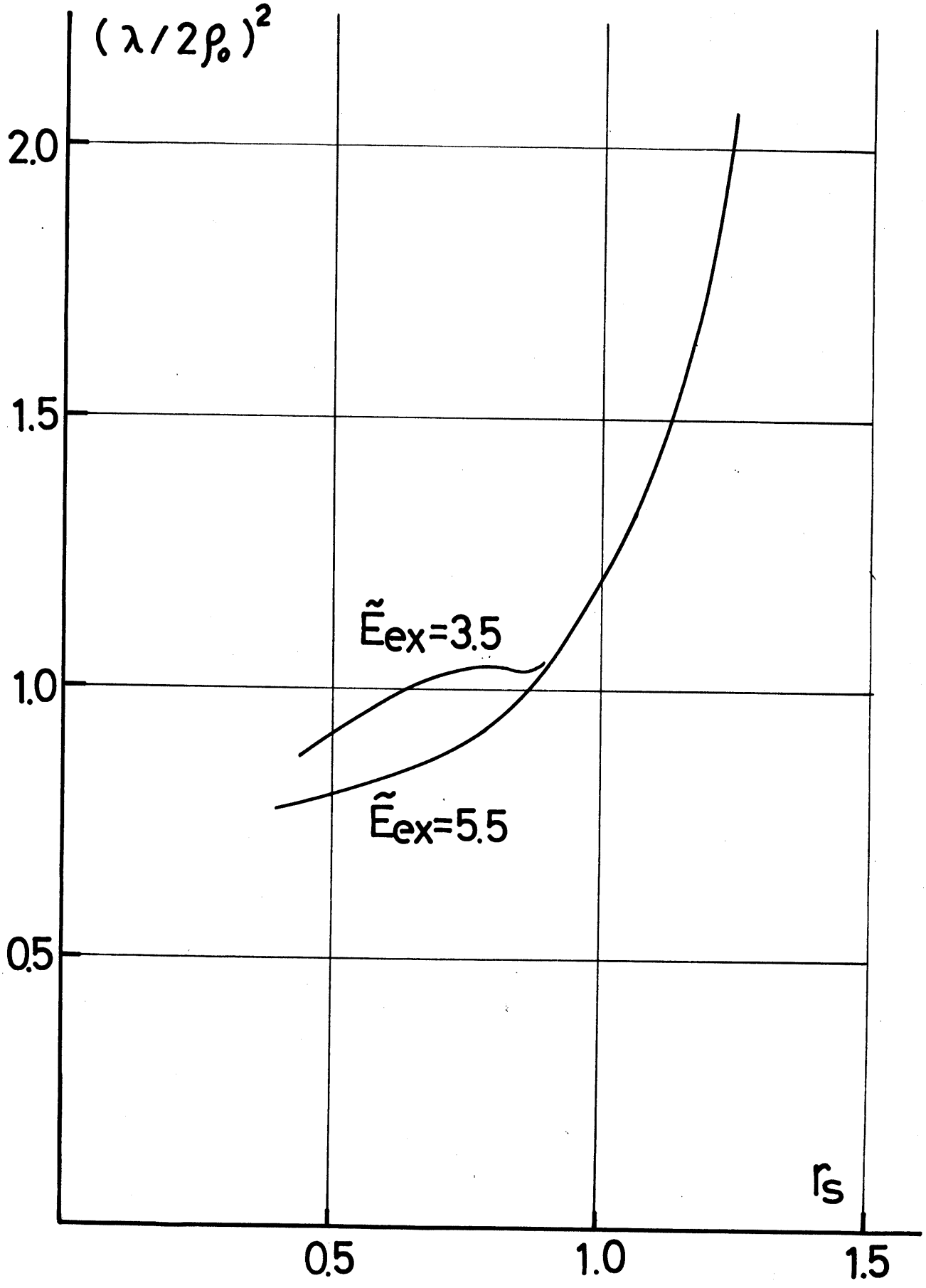

FIG. 3

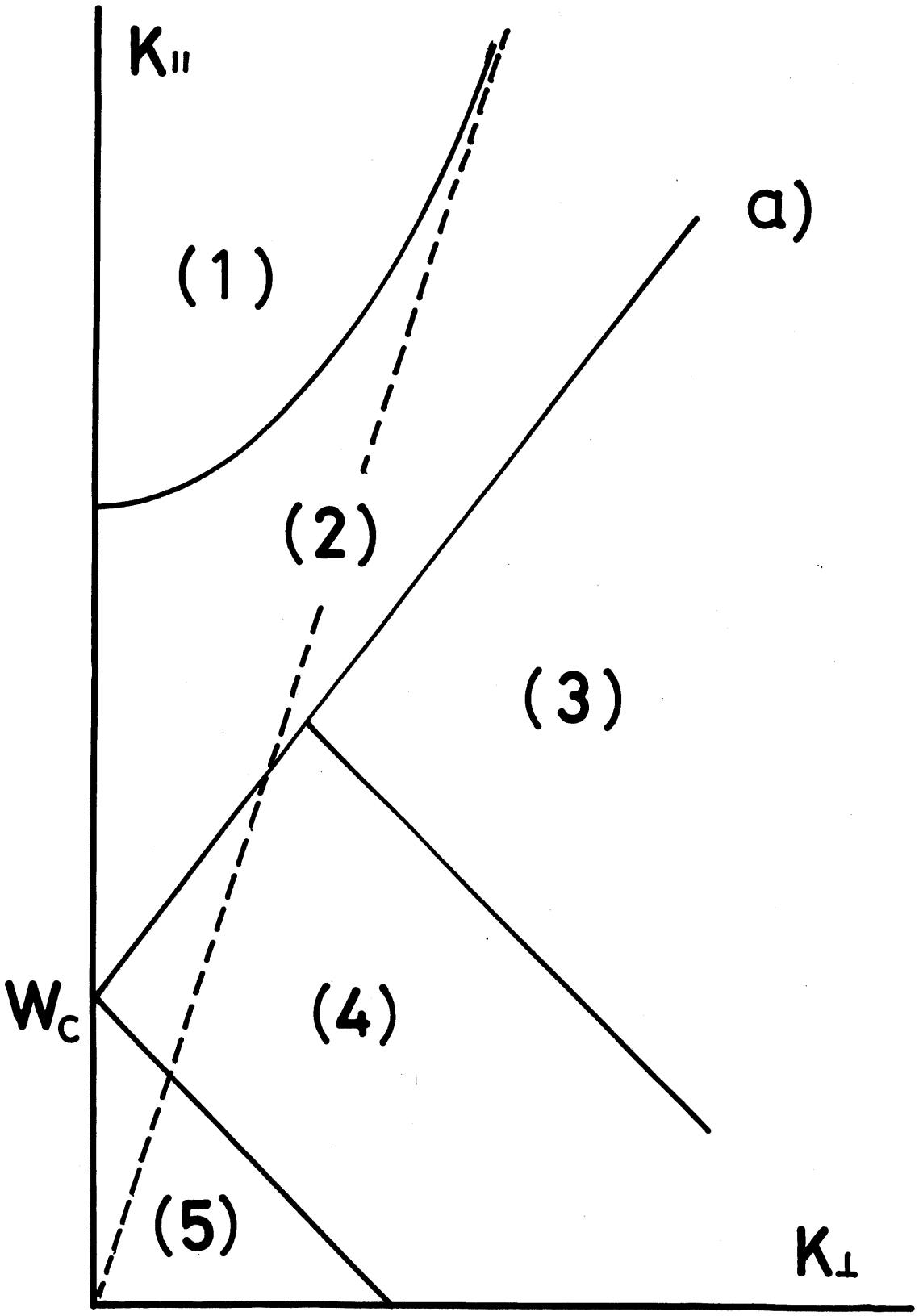

FIG. 4

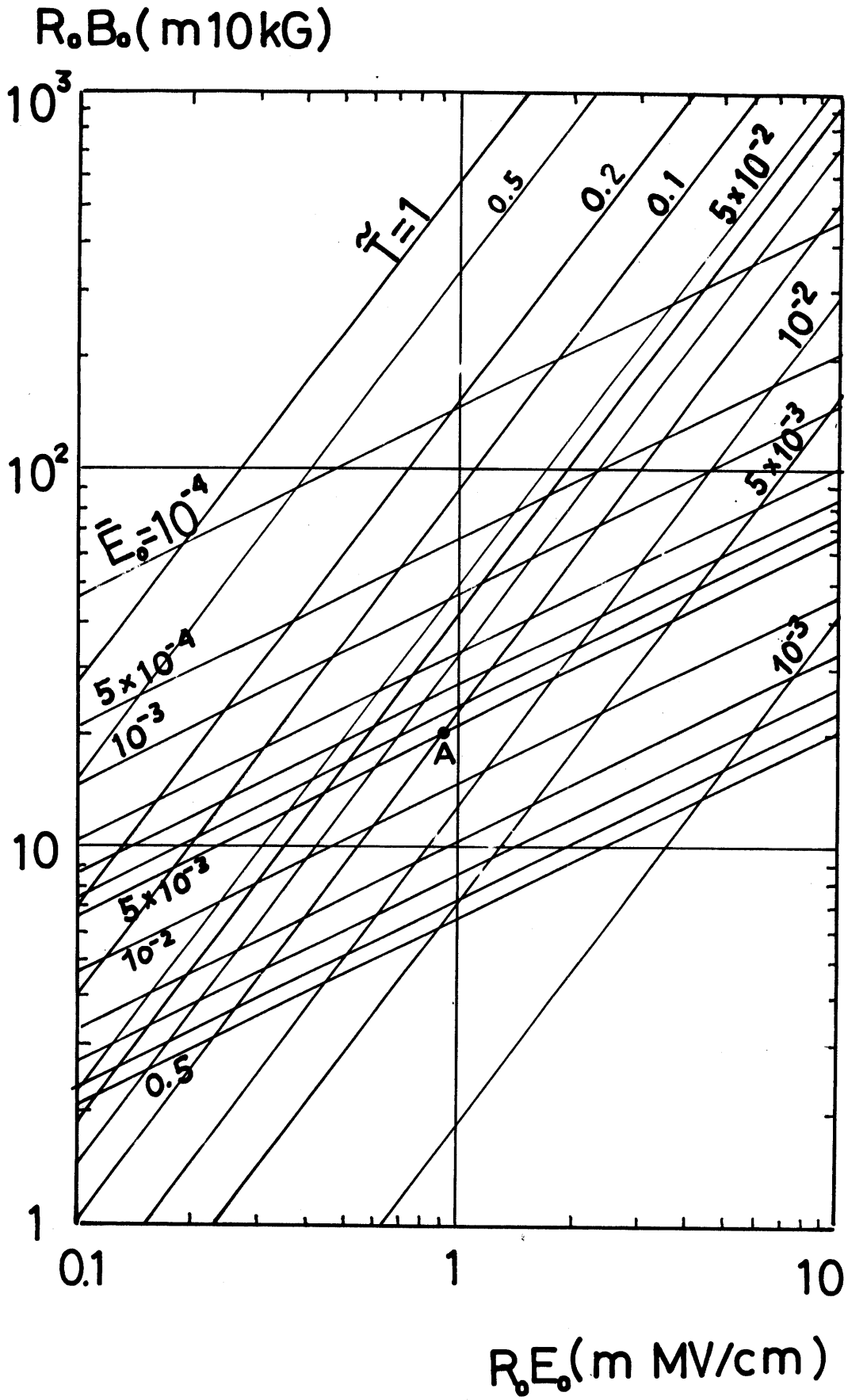
R₀B₀(m10kG)
10³
10²
10
1
0.1
1
10
R₀E₀(m MV/cm)
T̃=1
0.5
0.2
0.1
5×10⁻²
10⁻²
5×10⁻³
10⁻³
Ẽ₀=10⁻⁴
5×10⁻⁴
10⁻³
5×10⁻³
10⁻²
0.5
A

FIG. 5

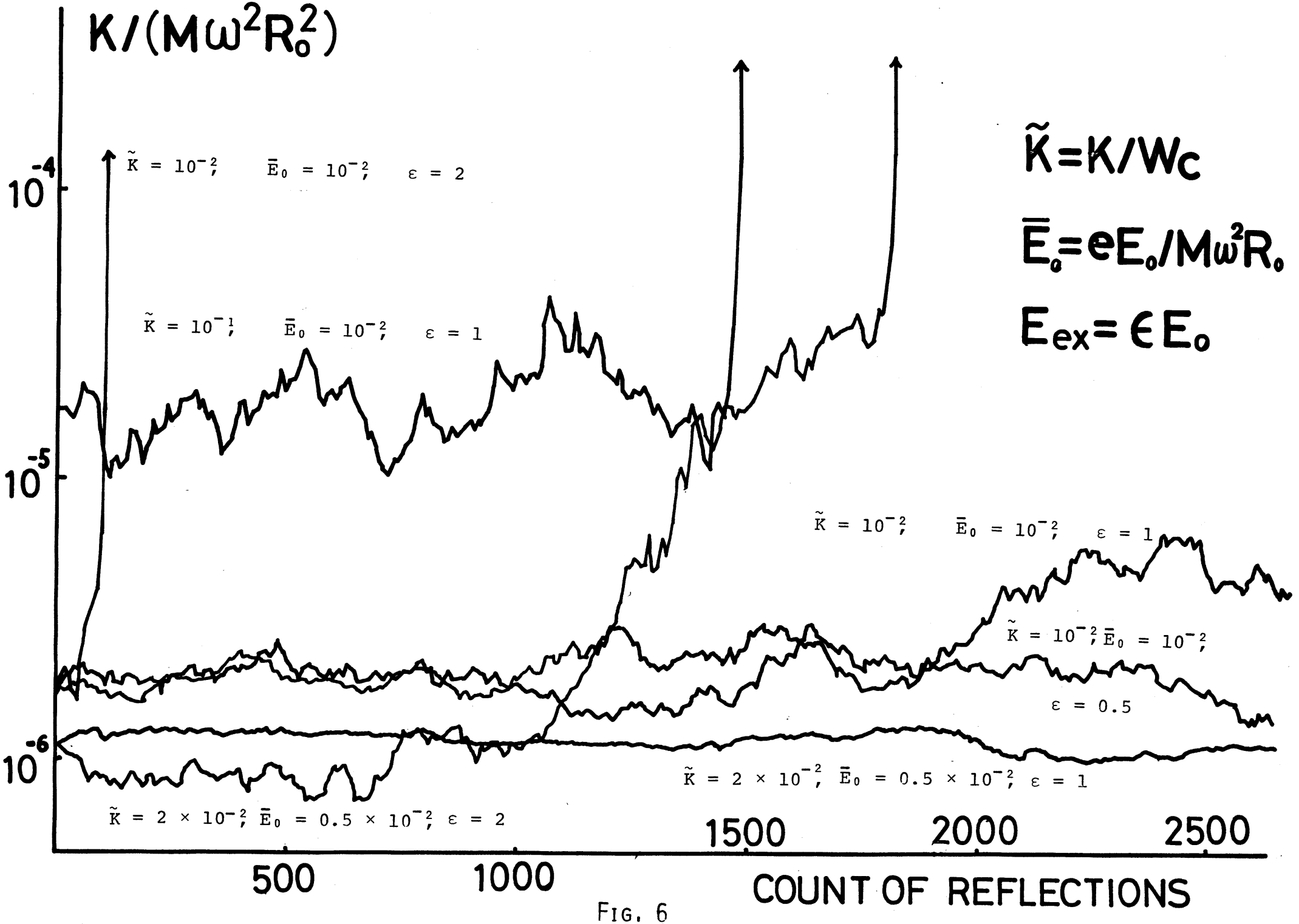
$K/(M\omega^2R_o^2)$
$\tilde{K}=K/W_c$
$\bar{E}_o=eE_o/M\omega^2R_o$
$E_{ex}=\epsilon E_o$
10^{-4}
10^{-5}
10^{-6}
$\tilde{K} = 10^{-2}$; $\bar{E}_0 = 10^{-2}$; $\varepsilon = 2$
$\tilde{K} = 10^{-1}$; $\bar{E}_0 = 10^{-2}$; $\varepsilon = 1$
$\tilde{K} = 10^{-2}$; $\bar{E}_0 = 10^{-2}$; $\varepsilon = 1$
$\tilde{K} = 10^{-2}$; $\bar{E}_0 = 10^{-2}$; $\varepsilon = 0.5$
$\tilde{K} = 2 \times 10^{-2}$; $\bar{E}_0 = 0.5 \times 10^{-2}$; $\varepsilon = 1$
$\tilde{K} = 2 \times 10^{-2}$; $\bar{E}_0 = 0.5 \times 10^{-2}$; $\varepsilon = 2$
500
1000
1500
2000
2500
COUNT OF REFLECTIONS

FIG. 6

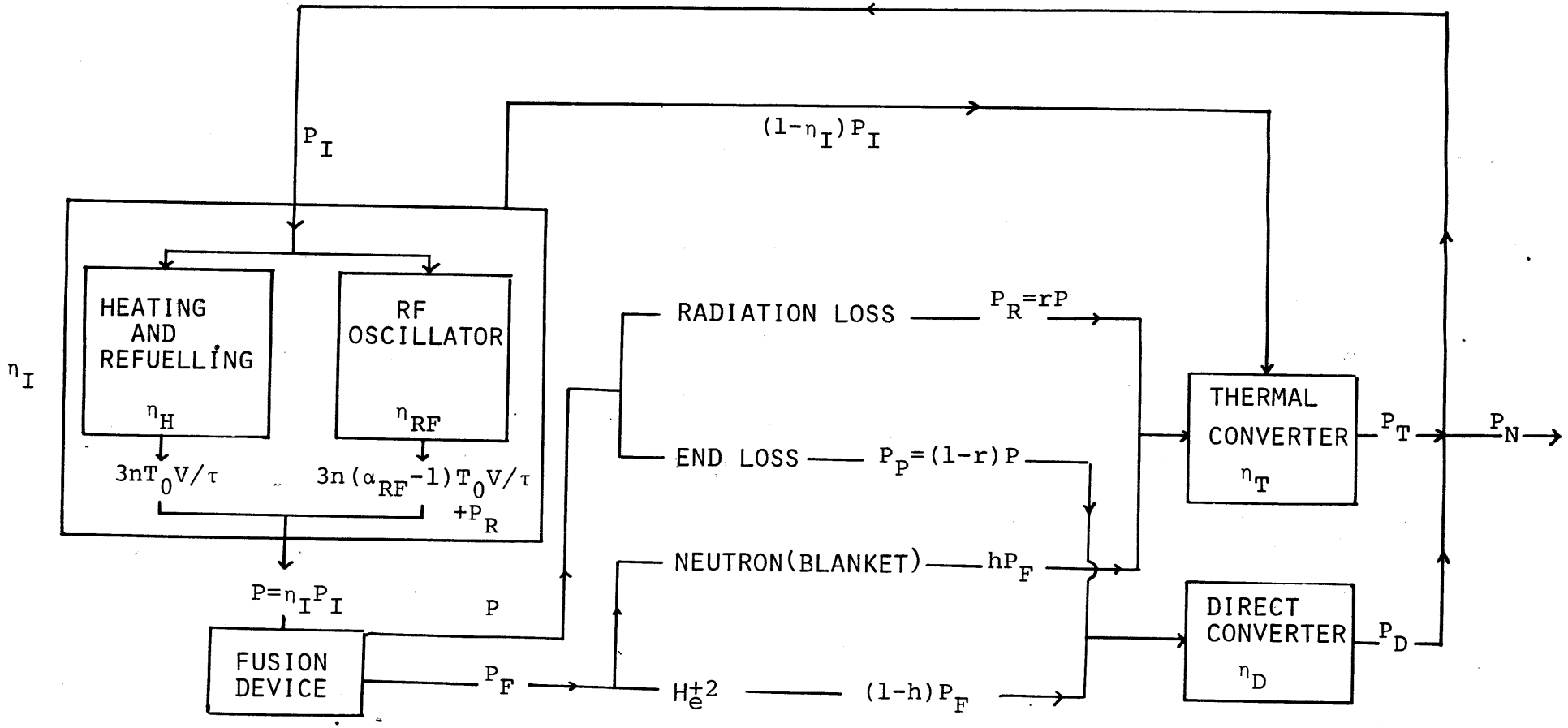
P_I
$(1-\eta_I)P_I$
η_I
HEATING AND REFUELLING
η_H
RF OSCILLATOR
η_{RF}
$3nT_0V/\tau$
$3n(\alpha_{RF}-1)T_0V/\tau$
$+P_R$
$P=\eta_I P_I$
P
FUSION DEVICE
P_F
RADIATION LOSS
$P_R=rP$
END LOSS
$P_P=(1-r)P$
NEUTRON(BLANKET)
hP_F
H_e^{+2}
$(1-h)P_F$
THERMAL CONVERTER
η_T
P_T
DIRECT CONVERTER
η_D
P_D
P_N

FIG. 7